Polymer distribution in silica aerogels impregnated with siloxanes by ^1H nuclear magnetic resonance imaging

Leoncio Garrido*, Jerome L. Ackerman and James M. Vevea
NMR Center, Department of Radiology, Massachusetts General Hospital and Harvard Medical School, 149 13th Street, Charlestown, MA 02129, USA

and James E. Mark and Shuhong Wang
Department of Chemistry and The Polymer Research Center, University of Cincinnati, Cincinnati, OH 45221, USA
(Received 15 February 1991; revised 29 April 1991; accepted 15 July 1991)

Polymer-modified aerogel samples were prepared by vacuum impregnation of silica aerogels with dimethylsiloxane–vinylmethylsiloxane copolymers. The specimens were characterized by ^1H nuclear magnetic resonance (n.m.r.) relaxation measurements. The effects of the polymer molecular weight, irradiation and aerogel density upon the spin–lattice (T_1) and spin–spin (T_2) relaxation times were studied. Significant reduction was observed in the T_2 values owing to increases in both aerogel and crosslink densities. ^1H n.m.r. images reveal a high degree of heterogeneity in the samples. Distribution maps of the polymer–silica interactions and crosslink density are obtained.

(Keywords: aerogels; silica; siloxanes; nuclear magnetic resonance imaging; impregnation)

INTRODUCTION

During the past 25 years, sol–gel processes have been extensively studied as alternatives to existing preparation methods for glasses and ceramics[1,2]. The main driving force has been the possibility of synthesizing these materials at low temperatures compared with the high-temperature process required by glass melting or firing. However, other advantages have resulted from the sol–gel methods besides the low processing temperatures, i.e. homogeneous distribution of all reactants and additives by liquid mixing, easy control of properties like viscosity for further manufacturing procedures, starting materials with high purity, preparation of hybrid materials by incorporation of organic components into inorganic matrices, etc. All of these have led to the preparation of new composite materials with improved and often unexpected physical and chemical properties. For example, the simultaneous growth of both polymer and silica networks has produced materials with good optical properties and very different mechanical behaviour (i.e. more flexible) compared to pure sol–gel silica glasses[3,4]. In these composites, the two phases (microscopic organic and inorganic clusters) are intimately connected to each other in a single macroscopic structure.

Other composites have been obtained by interpenetrating an already formed three-dimensional matrix with an *in situ* grown network. Thus, extensive work has been carried out to study the reinforcement of elastomers, in particular polydimethylsiloxane (PDMS)[5] and polyisobutylene (PIB)[6] networks, by *in situ* precipitated silica. Similarly, but now with the inorganic matrix as the original structure, Pope and coworkers[7] have studied the effect of composition upon optical and mechanical properties of silica gels impregnated with poly(methyl methacrylate) (PMMA).

The mechanisms controlling the final properties of the composite materials are often not well understood. It is almost certain that these properties would depend, in a complex way, upon the intrinsic characteristics of each phase (organic and inorganic), their relative size and distribution and the interactions between them. Because of the sensitivity of nuclear magnetic resonance (n.m.r.) to the molecular motions and chemical composition, this technique is ideally suited for the characterization of these materials. Moreover, with n.m.r. imaging techniques it is possible to produce tomographic images of three-dimensional objects[8]. The visual contrast in these images is based upon spatial variations of n.m.r. parameters such as relaxation times (spin–lattice, T_1; spin–spin, T_2; etc.), concentration of the nuclei being observed and chemical composition of the sample.

The n.m.r. imaging methods that we have developed to monitor ceramics processing[9–13] and other composites[14,15] (natural or synthetic) show that n.m.r. imaging could be an extremely useful tool for non-destructive evaluation of materials. In previous work, we have used n.m.r. spectroscopy and imaging techniques for the characterization of PDMS networks reinforced with *in situ* precipitated silica[16]. The extent and uniformity of the process is assessed by mapping the organic phase distribution (PDMS) and the degree of alkoxide hydrolysis in the specimens.

We report here the results obtained on polymer-modified silica aerogels using n.m.r. imaging to measure

* To whom correspondence should be addressed

0032-3861/92/091826-05

the distribution of siloxane copolymer in the samples. We have studied the effect of irradiation and aerogel density on the n.m.r. relaxation parameters of the copolymers. The ^{1}H n.m.r. images obtained provide a measure of molecular mobility that might be related to the spatial variation of crosslink density and silica–polymer interactions throughout the composite.

EXPERIMENTAL

Silica aerogels were prepared at Sandia National Laboratories according to the procedure described in ref. 17. Two types of samples, A and B, were synthesized with densities of 0.150 and 0.414 g cm^{-3}, respectively. Selected samples of both types (A and B) were vacuum impregnated with dimethylsiloxane–vinylmethylsiloxane copolymers having number-average molecular weight M_n, and chemical composition as shown in *Table 1*. During the course of the impregnation some specimens were fragmented.

A set of samples prepared as described were irradiated with a γ source at near room temperature under a nitrogen atmosphere. The degree of crosslinking was effectively varied by changing the radiation dosage and the concentration of vinyl groups in the copolymers. Also, samples containing only polymer were crosslinked under the same conditions.

Table 1 Characteristics of polysiloxanes

Sample ref.	y^a (%)	$M_n{}^b$	M_w/M_n
I	1.0	6200	3.42
II	1.0	13900	3.09
III	7.5	17400	2.93

^{a}Structure is $-[Si(CH_3)_2-O]_x-[Si(CH_3)(CH{=}CH_2)-O]_y-$
^{b}Number-average molecular weight (g mol^{-1})

The n.m.r. experiments were performed at room temperature in a Bruker MSL 400 spectrometer/imager equipped with an Oxford 9.4 T (^{1}H resonance frequency of 400.13 MHz) 8.9 cm vertical-bore superconducting magnet. The r.f. coil used was a saddle type with a diameter of 10 mm and its longitudinal axis parallel to the static magnetic field. The pulsed gradient amplitudes in the imaging experiments varied between 4 and 22 G cm^{-1}.

Bulk ^{1}H T_1 and T_2 measurements were carried out using inversion recovery and Hahn spin-echo sequences, respectively. The results are shown in *Table 2*. The inversion time in the inversion recovery sequence was varied between 0 and 10 s. The echo time *TE* (time between the 90° r.f. pulse and the centre of the echo) in the spin-echo sequence ranged from 10^{-4} to 1 s. The repetition time *TR* was 10 s in both cases, more than five times T_1.

^{1}H n.m.r. images of the polymer-modified aerogels were obtained using two-dimensional Fourier transform (2DFT) spin-echo techniques with *TE*s of the order of 2.8 and 123 ms. The selective excitation of a slice throughout the sample 500 μm thick was achieved with a 1 ms sinc-function amplitude-modulated r.f. pulse. The pulse sequence *TR* was typically 1 s and the total imaging time was 8.6 min. The digital resolution was 128 X by 128 Y pixels of 115 and 130 μm, respectively.

The image processing was performed on a SUN 4 workstation using software developed at the MGH NMR Center.

RESULTS AND DISCUSSION

The analysis of the ^{1}H T_1 data for all samples was carried out assuming the presence of only one component (a monoexponential function) since no evidence was found for biexponential spin–lattice relaxation behaviour. The

Table 2 Radiation dosage, T_1 and T_2 values for polysiloxanes and polymer-modified silica aerogels

Sample^a	Radiation (Mrad)	T_1 (s)	T_{2S} (ms)	$f_S{}^b$	T_{2L} (ms)
I	–	1.35 (0.02)^c	–	–	316 (6)^c
II	–	1.35 (0.01)	–	–	182 (8)
III	–	1.35 (0.01)	–	–	194 (10)
I + A	–	–	21 (17)^c	0.10 (0.06)^c	149 (11)
II + A	–	–	29 (7)	0.34 (0.09)	111 (12)
III + A	–	–	27 (9)	0.35 (0.12)	118 (17)
II + B	–	–	16 (2)	0.71 (0.11)	60 (17)
I	15	–	13.4 (0.6)	0.55 (0.010)	308 (12)
I	20	–	7.2 (0.3)	0.58 (0.007)	317 (13)
II	15	–	6.4 (0.3)	0.69 (0.008)	268 (17)
II	20	–	4.9 (0.2)	0.74 (0.007)	286 (20)
III	8	–	9.4 (0.3)	0.61 (0.008)	270 (11)
I + A	15	1.31 (0.007)	5.0 (0.2)	0.60 (0.01)	120 (7)
I + A	20	1.28 (0.01)	3.7 (0.2)	0.70 (0.02)	112 (14)
II + A	15	1.34 (0.01)	5.8 (0.7)	0.47 (0.03)	91 (10)
II + A	20	1.27 (0.04)	2.0 (0.09)	0.76 (0.01)	77 (12)
III + A	8	1.26 (0.006)	4.5 (0.2)	0.64 (0.02)	94 (8)
II + B	15	1.23 (0.007)	4.6 (1.0)	0.47 (0.07)	37 (6)

^{a}A and B denote silica aerogels with densities of 0.150 and 0.414 g cm^{-3}, respectively. See *Table 1* for notation on polymers
^{b}Fraction of component with shorter T_2 ($f_S + f_L = 1$)
^{c}The numbers in parentheses represent the standard deviation

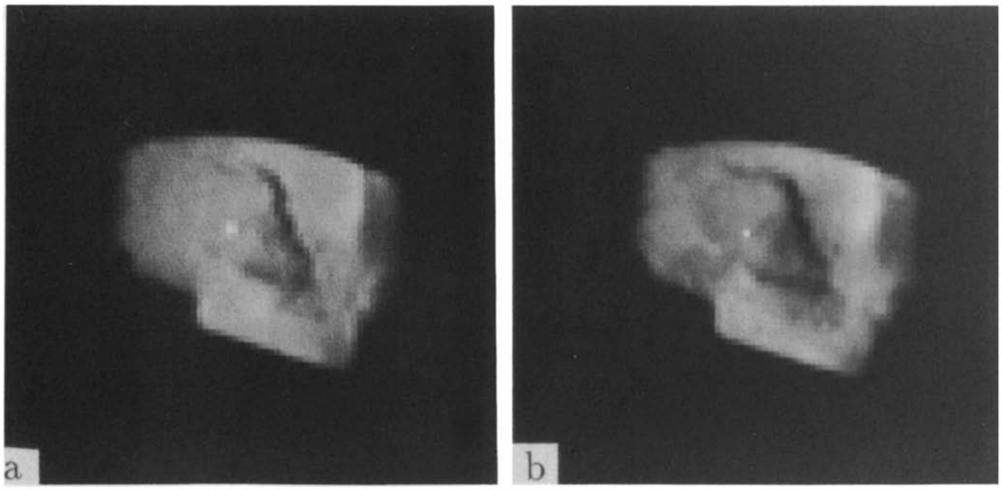

Figure 1 ^{1}H n.m.r. images of sample II + A (0 Mrad) obtained with a two-dimensional spin-echo sequence having a *TE* of (a) 2.82 and (b) 122.6 ms. *TR* was 1 s in both cases. Selective excitation was used to define a 500 μm slice thickness through the sample. The resolution is 128 *X* by 128 *Y* pixels of 115 and 130 μm, respectively, in both cases. The time required to acquire the data for each image was 8.6 min

results are shown in *Table 2*. As expected, the presence of radiation-induced crosslinks[18,19] and the silica–polymer chain interaction[16] seem to leave unperturbed the n.m.r. spin–lattice relaxation mechanism of the copolymer. T_1 is sensitive to molecular motions occurring at frequencies near the resonance frequency. In this case, the motion probably consists of reorientation of the methyl group C_3 axis by rotation of main-chain segments not involving many chain atoms[20,21]. The methyl group rotation about the Si–C bond is too fast at room temperature to provide an effective contribution to T_1 (ref. 20). The T_1 values obtained are similar to those of unfilled and reinforced PDMS model networks with a wide range of molecular weight between crosslinks[16,22].

The behaviour of the n.m.r. transverse relaxation in these composite materials is very complex. T_2 is generally associated with the low-frequency motions involving large portions of a macromolecule. Therefore, it will be very sensitive to any factor affecting the number of configurations available for a molecule. This has been confirmed in various studies on PDMS[16,18,19,23]. In the present work, the formation of crosslinks by radiation and the presence of the silica aerogel will tend to reduce the molecular mobility of the siloxane copolymer, making its T_2 short. An apparent two-component model gives the best fit to the experimental results except for the copolymer melts (uncrosslinked). Although the siloxane melt samples are polydisperse, the T_2 relaxation process is well described with a monoexponential function instead of a discrete distribution of T_2 values, as could be expected. The values obtained for the various samples are shown in *Table 2*.

The irradiated copolymers show a biexponential behaviour, which indicates the presence of two major components contributing to the n.m.r. signal. One might be attributed to polymer strands that are part of the three-dimensional network and the other to the polymer chains not crosslinked. As expected, when the radiation dosage is increased, the fraction of the component with short T_2 increases and T_{2S} is reduced. The fraction attributed to the free polymer has T_2 values similar to those of the polymer melts.

The other factor limiting the segmental mobility of the polymer chains in the samples studied is the polymer–silica interaction. The T_2 data fit a two-component model well and clearly show a decrease in T_2 with an increase in aerogel density. The siloxane molecular mobility is significantly hindered in the aerogel as compared to that in the melt. An increase in polymer molecular weight does not significantly affect the T_2 values of the copolymers but the fraction of the component with short T_2 increases. The irradiation of these samples increases the polymer fraction with short T_2 and further reduces the value of T_{2S}.

The effect of radiation and siloxane–silica interactions upon the copolymer n.m.r. relaxation times might be mapped by ^{1}H n.m.r. imaging. *Figure 1* shows two 500 μm thick tomograms of a non-irradiated sample II + A (see *Table 2* for sample reference). The images were obtained with a two-dimensional spin-echo sequence having *TE*s of (a) 2.82 and (b) 122.6 ms. The rest of the experimental conditions were the same for both images. At the longest echo time, the contribution of the short T_2 fraction is only 2% and, therefore, the signal intensity of the image reflects mainly the distribution of the component with higher molecular mobility.

The lack of uniformity in signal intensity throughout the specimens is clearly visible in these images and it seems to indicate a heterogeneous distribution of both polymer and polymer–silica interactions. Taking into account the measured T_{2S} for each sample and with the appropriate linear combination of two images acquired with different *TE*s, it is possible to calculate a new image in which the brightness represents the fraction of the component of interest. *Figure 2* shows a computed image obtained as described previously using the results seen in *Figures 1a* and *1b*. The areas with high signal intensity represent the regions with decreased polymer molecular mobility owing to an increased aerogel density.

The n.m.r. images of the irradiated samples are similar in appearance to those of the non-irradiated polymer-impregnated aerogels. In *Figures 3a* and *3b* are shown in ^{1}H n.m.r. images of a sample II + A (15 Mrad) that were acquired with the same conditions as *Figures 1a* and *1b*, respectively. The variations in signal intensity in these images are real, and not due to experimental artifacts. This is confirmed by rotating the sample physically in the n.m.r. probe. *Figures 4a* and *4b* show two images of a sample III + A (8 Mrad) that were taken

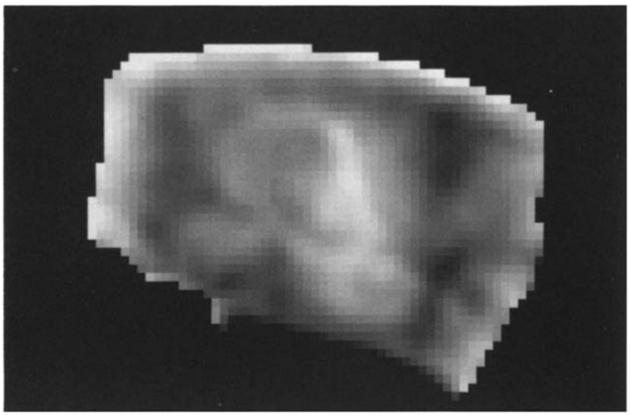

Figure 2 Spatial distribution of the polymeric component with short T_2 in the sample II + A (0 Mrad). This calculated image is the result of a linear combination of the n.m.r. images shown in *Figure 1*

with the same conditions and similar to those used in *Figure 1b*. In *Figure 4b* the sample has been rotated 90° with respect to its original position in *Figure 4a*. The rotation of the specimen was around the axis perpendicular to the selected slice (imaging plane through the sample). The local differences in signal intensity highlight the regions with high molecular mobility. For the purpose of comparison, *Figure 5* shows a ^{1}H n.m.r. image of a pure polymer sample III crosslinked in the same conditions as those used for the previous aerogel sample. The experimental parameters of the n.m.r. imaging experiment were the same as *Figure 4a*. No edge effects are observed and the signal intensity across the sample is relatively uniform. In fact, the standard deviation about the mean signal intensity value for the entire sample is only 6% while that for the sample section shown in *Figure 4a* is 33%. This might indicate that the crosslinking reaction is quite uniform in the examined section of the sample with the current experimental conditions.

The distribution map of the component with short T_2 corresponding to the sample II + A (15 Mrad) is shown in *Figure 6*. The non-uniformity in brightness throughout the specimen is mainly due to variations in aerogel density

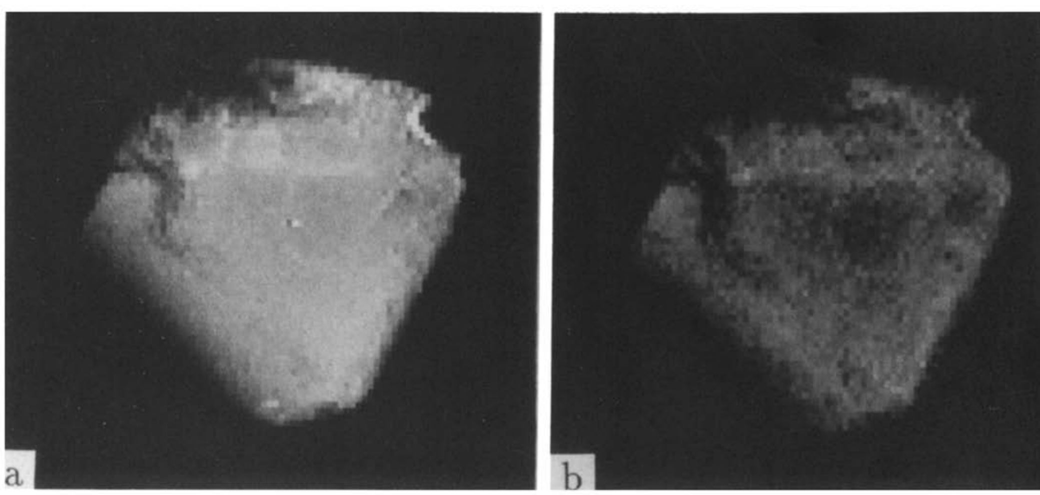

Figure 3 ^{1}H n.m.r. images of sample II + A (15 Mrad), taken with the same experimental conditions as for *Figures 1a* and *1b*, respectively. A significant variation of n.m.r. signal intensity across the sample is observed with increased contrast (differences in brightness) at long *TE*

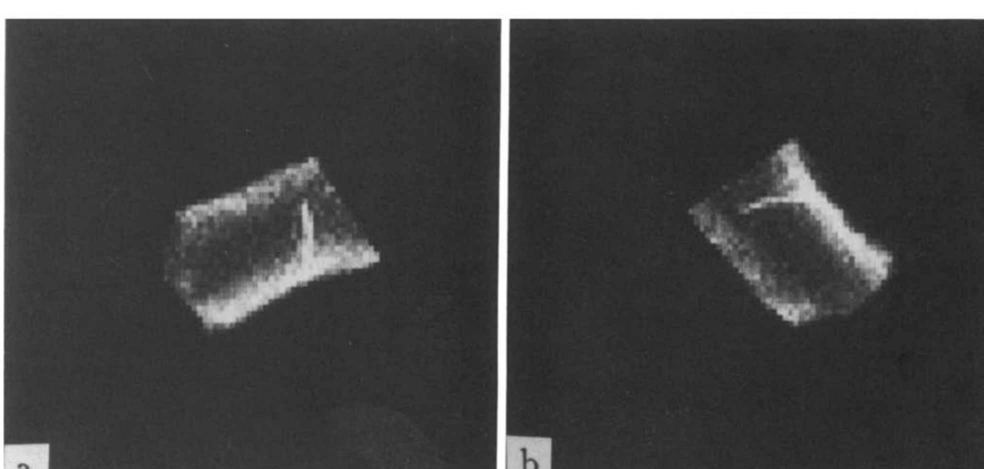

Figure 4 ^{1}H n.m.r. images of sample III + A (8 Mrad) taken with imaging parameters similar to those in *Figure 1b*. In (b) the sample was physically rotated 90° with respect to its original position shown in (a). It is clear that the differences in n.m.r. signal intensity observed in these experiments are not due to experimental artifacts

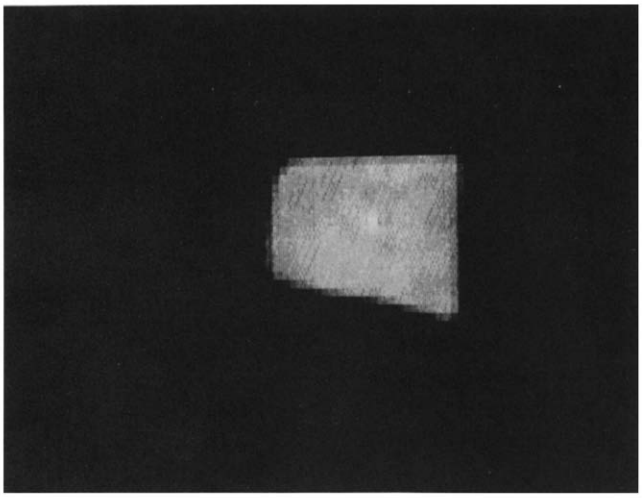

Figure 5 [1]H n.m.r. image of a polymer sample III (8 Mrad) taken with imaging parameters similar to those in *Figure 4*. No edge artifacts are observed

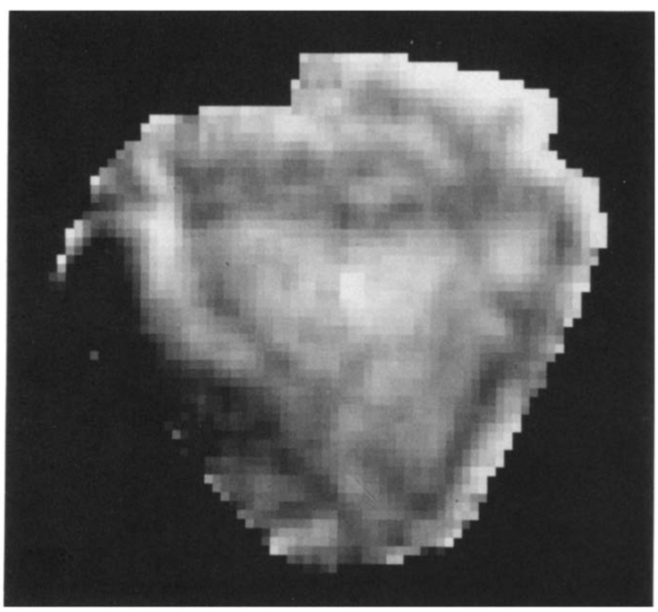

Figure 6 Calculated map of the component with short T_2 corresponding to sample II + A (15 Mrad). It reflects, indirectly, the distribution of crosslinks and polymer–silica interactions throughout the specimen

since the irradiation process, as mentioned above, is relatively uniform at the resolution of the n.m.r. imaging experiments.

CONCLUSIONS

Proton n.m.r. relaxation times have been measured for the various types of polymers and aerogels prepared. The spin–spin relaxation time of the siloxane copolymers is significantly sensitive to the presence of silica and crosslinks. The aerogel structure hinders the long segmental macromolecular motions shortening the T_2 of the copolymer. An increase in the aerogel density decreases T_2. The sample irradiation affects T_2 of the siloxanes as well, but its effect on T_2 is larger than the polymer–silica interaction. This is because the chemical bonding between polymer chains imposes a more severe reduction in the macromolecular degrees of freedom.

The n.m.r. imaging results demonstrate the usefulness of this technique for the characterization of polymer-modified silica aerogels. ^{1}H n.m.r. images reveal inhomogeneities in the samples. The local variations in signal intensity (visual contrast) are highlighted with proton density and T_2-weighted imaging pulse sequences suggesting that the changes seen in the image may be closely related to variations in both the concentration and the mobility of the polymer. The regions with reduced signal intensity seem to grow in size as TE increases, which might indicate high aerogel density for those regions (larger polymer–silica interactions). The calculated images display separately maps of the free polymer and the distributions of siloxane–silica interactions and crosslink density.

ACKNOWLEDGEMENTS

This work was supported in part by NSF grant DMR 89-18002, Division of Materials Research, Polymers Group; Army Research Office grant ARO DAAL-03-90-G0131; NIH grant RR03264; and the MGH NMR Center. The authors express their gratitude to Dr Dale W. Schaefer (Sandia National Laboratories) for providing the silica aerogel samples.

REFERENCES

1 Mackenzie, J. D. and Ulrich, D. R. 'Ultrastructure Processing of Advanced Ceramics', Wiley, New York, 1988
2 Brinker, C. J., Clark, D. E. and Ulrich, D. R. 'Better Ceramics Through Chemistry', Materials Research Society, Mater. Res. Soc. Proc. 121, Pittsburgh, 1988
3 Huang, H., Orler, B. and Wilkes, G. L. *Macromolecules* 1987, **20**, 1322
4 Huang, H., Wilkes, G. L. and Carlson, J. G. *Polymer* 1989, **30**, 2001
5 Mark, J. E. *Br. Polym. J.* 1985, **17**, 144, and references therein
6 Sun, C. and Mark, J. E. *J. Polym. Sci., Polym. Phys. Edn.* 1987, **25**, 1561
7 Pope, E. J. A., Asami, M. and Mackenzie, J. D. *J. Mater. Res.* 1989, **4**, 1018
8 Mansfield, P. and Morris, P. G. 'NMR Imaging in Biomedicine', Suppl. 2, 'Advances in Magnetic Resonance', Academic Press, New York, 1982
9 Ackerman, J. L., Ellingson, W. A., Koutcher, J. A. and Rosen, B. R. 'Nondestructive Characterization of Materials II', Plenum, New York, 1987, p. 129
10 Ackerman, J. L., Garrido, L., Ellingson, W. A. and Weyand, J. D. 'Nondestructive Testing of High-Performance Ceramics', American Ceramics Society, 1988, p. 88
11 Garrido, L., Acjerman, J. L., Ellingson, W. A. and Weyand, J. D. *Ceram. Eng. Sci. Proc.* 1988, **9**, 1465
12 Garrido, L., Ackerman, J. L. and Ellingson, W. A. *J. Magn. Reson.* 1990, **88**, 340
13 Moore, J. R., Garrido, L. and Ackerman, J. L. *Ceram. Eng. Sci. Proc.* 1990, **11**, 1302
14 Ackerman, J. L. and Garrido, L. 'Seventh Annual Meeting, Society of Magnetic Resonance in Medicine', 1988, p. 195
15 Garrido, L., Ackerman, J. L. and Mark, J. E. *Mater. Res. Soc. Symp.* 1990, **171**, 65
16 Garrido, L., Mark, J. E., Sun, C. C. and Ackerman, J. L. *Macromolecules* 1991, **24**, 4067
17 Schaefer, D. W., Brinker, C. J., Wilcoxon, J. P., Wu, D. Q., Phillips, J. C. and Chu, B. *Mater. Res. Soc. Symp. Proc.* 1988, **121**, 691
18 Folland, R. and Charlesby, A. *Radiat. Phys. Chem.* 1977, **10**, 61
19 Folland, R., Steven, J. H. and Charlesby, A. *J. Polym. Sci., Polym. Phys. Edn.* 1978, **16**, 1041
20 Powles, J. G., Hartland, A. and Kail, J. A. E. *J. Polym. Sci.* 1961, **55**, 361
21 Cuniberti, C. J. *J. Polym. Sci. (A2)* 1970, **8**, 2051
22 Garrido, L., unpublished data
23 Cohen-Addad, J. P., Viallat, A. and Huchot, P. *Macromolecules* 1987, **20**, 2146